ACCELERATING STRUCTURE OF THE CERN NEW 50 MeV LINAC

D.J. Warner
CERN, Geneva, Switzerland

Summary

The design of the post-coupled Alvarez structure is presented with emphasis on features which are novel and critical especially as regards acceleration of high currents (150 mA) to 50 MeV. Among topics treated are the sequence of computational techniques leading from unit cell (e.m. field) calculations to dynamics of the complete linac, and model measurements which justify the drift-tube girder support approach and our particular post-coupler arrangement.

Introduction

In this paper we outline the procedures used for the linac structure design, concentrating mainly on the physical aspects (e.g. the results of computations and measurements) which specified the structure in sufficient detail to allow the engineering designs to be developed and their merits considered.

A complementary paper[1] will treat details of the more analytical side of the beam matching and dynamics with space charge; here we limit the discussion to the selection of a set of parameters (summarized in Table 1). The 1973 design study report[2] treated topics in a preliminary manner leaving options open, e.g. on the dynamics of Tank I and on the structure stabilization, but the general approach used there remains valid.

Structure Design Tools

The physical design is an iterative procedure involving the specifications of the input beam, mechanical possibilities, quadrupole magnet limitations, RF power limitations as well as the use of "tools" (mainly computer programs) to derive the electromagnetic, dynamics, and dimensional information presented here.

The main computer programs are described below:

CLASL [3]

This cavity computation program starts from the unit cell dimensions as boundary conditions [diameter (D), length (L), gap (g), drift-tube diameter (d), aperture diameter (HD), and profile radii (r and r_{hc})] and uses a compound numerical and analytical procedure to solve

$$\frac{\partial^2 U}{\partial r^2} - \frac{1}{r}\frac{\partial U}{\partial r} + \frac{\partial^2 U}{\partial z^2} + \left(\frac{\omega}{c}\right)^2 U = 0$$

to give values of $U = rH_\phi$ at a large number (10,000 to 20,000) of discrete points. Quantities derived from the set of U include

a) frequency perturbations due to support stem and post coupler;

b) stored energy; dissipations on copper surfaces, Q, shunt impedance and electric fields on the axis and drift-tube surface all normalized to a mean axial electric field of 1 MVm^{-1};

c) dynamics coefficients[4,5] such as T, k(dT/dk), $k^2(d^2T/dk^2)$, S, etc., corresponding to a reference particle with $\beta = v/c = L/\lambda$ and $k = 2\pi/L = \omega/\beta c$.

GENLIN [5]

This program generates the linac cell lengths by tracing the axial synchronous particle, given the dynamics data from CLASL, the mean electric field, and synchronous phase ϕ_s. In addition, the program calculates the dynamics coefficients corresponding to every cell for subsequent use (see under MAPRO 1). Recent improvements in GENLIN allow us to interpolate the dynamics data from a limited number of CLASL cells and to treat the electric field and synchronous phase as functions of longitudinal position.

ADAPT [6]

This program and its several variants (ADAPTEF, LINEF), all essentially calculate matching parameters (α, β) (in all phase planes) at the beginning of the linac and, assuming linear space charge forces, transfer the beam through one or more cavities maintaining the matched situation by adjustment of quadrupole gradients. Transversely, the emittance, quadrupole periodicity (+-+-) and the phase advance per focusing period μ^0 are specified. Longitudinally, the phase envelope $\widehat{\Delta\phi}$ is specified. The matching calculation is carried out for several currents incrementing by 10 to 25 mA between cases. For subsequent use in the more general dynamics programs (MAPRO 1 and MAPRO 2), α, β, and quadrupole gradients are punched out at beam currents 0 mA, 50 mA, 100 mA, and 150 mA. ADAPTEF and LINEF can also treat discontinuities between quadrupole batches and linac tanks.

MAPRO 1 [4]

The multiparticle beam simulation programs MAPRO 1 and MAPRO 2 were developed to study non-linear space charge dynamics in the linac using an expanded set of equations (cf. GENLIN) to treat the accelerating gap. Although it is slower than MAPRO 2, we prefer MAPRO 1 for studies on real linacs with general particle distributions at input (bunched beams). For comparison purposes, most of our studies have used a distribution which is uniform within a four-dimensional hyperellipsoid (transverse phase planes) and uniform within an ellipse in the longitudinal phase plane. After selecting the particle coordinates randomly as prescribed above, the raw distributions are corrected to fit the precise input matching parameters[7]. This procedure has been invaluable when comparing cases with different currents, focusing strengths, phase laws,

and/or distributions. Results can be in the form of scatter diagrams of phase plane projections or as graphs showing the evolution of beam envelopes ($\hat{x}$,$\hat{y}$, $\widehat{\Delta\phi}$) beam emittances, beam centroid phase, and energy error along the linac.

Design Procedure

As we do not know the actual cell dimensions until the design via GENLIN is complete, we have to compute a limited number of typical cells precisely, and in particular adjust the gap length to obtain the resonant frequency of 202.56 MHz to within ±50 kHz (also including the support stem and post-coupler perturbation). A total of 36 cells were calculated for the GENLIN dynamics data as representative of the (eventual) 128 cells in the linac.

Choice of Operating Parameters between 0.75 MeV and 10 MeV

A large synchronous phase angle ($|\phi_s| > 30°$) at 0.75 MeV is needed to contain a matched 150 mA beam, but on RF economy and dynamics grounds $|\phi_s|$ should be reduced as the energy increases. Thus to select from some possible laws of variation of ϕ_s we have computed several cases up to 10 MeV using GENLIN, ADAPT and MAPRO 1.

In GENLIN the dynamics coefficients were fitted by least squares to polynomials up to third degree in L and it was usually possible to obtain the r.m.s. deviation of the CLASL data points from the fitted curve to < 0.3%. As well as the imposed ϕ_s law, we specify the axial electric field. For ADAPT, we require the set of dynamics coefficients, cell lengths, accelerating fields and synchronous phases for each E, ϕ_s law treated by GENLIN. The bunching system and its associated focusing[8] can match the beam longitudinally and transversely over the useful range of $\widehat{\Delta\phi}$ (25° to 35°). This allows us to specify only the phase width $\widehat{\Delta\phi}$ of the bunch entering the linac and to derive, via ADAPT, the matched energy spread. The beam dimensions, required gradients, and stability can be obtained for the different ϕ_s laws with ADAPT; further studies on the initial values of α and β and the evolution of the beam matching and emittance are made with MAPRO 1.

With a constant μ structure, the MAPRO 1 graphical outputs of $\hat{x}$ and $\hat{y}$ clearly indicate beam mismatch by oscillations superimposed on a constant mean envelope. The ideal potential well (harmonic oscillator) assumed by ADAPT for the rather non-linear longitudinal motion produces matching coefficients which surprisingly need only slight modification (∿ 7% increase in β) to give acceptably small envelope oscillations in MAPRO 1. Thus we can make a preliminary choice of the ϕ_s law using ADAPT, as the input emittances and space charge limits are approximately defined. Firstly, we set a limit $\phi_s = -25°$ at 10 MeV to avoid longitudinal stability problems at higher energies. After eliminating constant $\phi_s = -30°$ (space charge limit < 150 mA) we considered:

a) $\phi_s = -40°$ to $-25°$, $\widehat{\Delta\phi}_{in} = 35°$

b) $\phi_s = -40°$ to $-25°$, $\widehat{\Delta\phi}_{in} = 25°$ and

c) $\phi_s = -35°$ to $-25°$, $\widehat{\Delta\phi}_{in} = 30°$.

Case (a) was far from the space charge limit but had an excessive longitudinal input emittance (35° × × 50 keV), and while (b) and (c) were similar as regards input emittance and its evolution, the latter had to be preferred as the smaller variation in ϕ_s would be more flexible during operation. Incidentally, there is the possibility with post couplers to vary the field tilt (hence the ϕ_s law) if necessary.

The above comparisons were made with the strongest focusing practicable with our quadrupole design. With a lower μ, there is a larger transverse emittance increase at 150 mA but less longitudinal increase. Experience with the 800 MeV booster synchrotron following the linac has shown that at 50 MeV the transverse emittance is more of a limitation than longitudinal emittance.

Design Procedure for Complete Linac

The following design conditions were introduced into GENLIN to define the complete linac.

i) Linac input energy = 0.750 MeV and output energy = 50 MeV.
ii) Division into three cavities with numbers of cells multiples of four giving 52, 44, and 32 cells, respectively (to allow higher periodicity structure compensation).
iii) Accelerating rate of 1.00 $MeVm^{-1}$ at 0.75 MeV.
iv) Mean axial electric field to increase linearly with distance in Tank I and to be constant in each of Tanks II and III.
v) Synchronous phase variation as β^{-x} between -35° and -25° in Tank I; $\phi_s = -25°$ in Tanks II and III.
vi) Continuity of synchronous energy (W_s), accelerating rate (dW_s/dz) and ϕ_s.

The electric fields were uniquely determined by the above conditions. This run of GENLIN determined the longitudinal dimensions for the entire linac with corresponding dynamics coefficients (T, S, etc.).

Now ADAPTEF (or LINEF) followed by MAPRO 1 could be run for the linac including matching across inter-tank spaces. Suppose we compare the increase in transverse emittance (ε_T) and longitudinal emittance (ε_L), for $\mu = 39°$, $\widehat{\Delta\phi}_{in} = 31°$ and normalized ε_T (0.75 MeV) = 2.6π mm mrad. For currents of 0 mA to 150 mA, ε_L (0.75) varies from 1.8π MeV° to 0.9π MeV°; but with the increase a function of current, ε_L (50) only varies from 1.7π MeV° to 2.0π MeV°. The increase in ε_T is negligible for all currents (< 15%). In practice, we would try to operate with constant ε_L (0.75) rather than constant $\widehat{\Delta\phi}$ (0.75). Use of the transverse parameters from ADAPT in MAPRO 1 usually gives good matching for many cases but there is sometimes deterioration (e.g. 20% envelope modulation) for low values of μ (15°-20°) and lower currents (presumably due to the proximity of the edge of the stability region). Longitudinally, a good match in Tank I with $\widehat{\Delta\phi}$ envelope modulation < 5% relative to the smooth adiabatic damping is increased to ∿ 15% (for 150 mA) at 50 MeV by the mismatch of the tank interspaces (especially between Tanks I and II).

We have confirmed that essentially the same behaviour in beam transverse emittance increase occurs with a more realistic distribution from the bunching simulation program (BUNCH 74 [7]). The stray particles outside the longitudinal acceptance caused less perturbation to the trapped beam than expected, mostly falling out of synchronism and being lost radially by 5 MeV.

On the basis of the above computations we were able to fix the mechanical dimensions.

Choice of Other Main Dimensions

Many dimensions for the initial runs of CLASL were based on preliminary data and calculations. In particular, the drift-tube profiles were essentially the same as at BNL and FNAL to house the same physical design of quadrupole magnet. With constant mean accelerating field and ϕ_s, the accelerating rate varies as the transit time factor, i.e. falling slightly as g/L increases. Thus the cavity diameters were chosen for an acceptable range of T along the cavity, implying smaller g/L and D than might have been chosen on RF economy grounds. Further dynamics studies (1974) eventually gave no clear reasons for changing from the 10 MeV and 30 MeV intertank energies favoured mainly for equality of the five RF amplifiers.

The computational work described in the previous sections culminated in the production via GENLIN of the longitudinal dimensions such as drift-tube lengths, gap lengths, positions of support stems (centred along drift tubes) relative to input plane of linac, and total tank lengths. The ideal position of RF feed loops is near the one-quarter and three-quarters position (centrally in Tank I) and this made the cavity section lengths rather unequal, ranging from 3.03 m to 3.54 m. Results of analyses and computations (ADAPT and MAPRO 1) indicated that intertank space should be the minimum consistent with diagnostic apparatus and mechanical and vacuum requirements (0.15 m and 0.20 m, respectively, between RF terminating planes).

The derived quantities from CLASL (normalized to 1 MVm^{-1}) are renormalized by the axial fields given by GENLIN, and then in the case of dissipations increased by 30% to allow for quality of copper surfaces and joints.

Details of Cavity and Component Design

Cavity Cross section

Consider the schematic cross section (Fig. 1) which shows the azimuthal positions of components. The girder which supports the drift tubes in a given tank section (used on the 3 MeV experimental linac[9]) is advantageous during installation, alignment, and maintenance, as the complete set of drift tubes can be removed through the slot. The slot geometry departs from the ideal circular section, but the frequency perturbation is typically only 300 kHz in 202.56 MHz. With the single vertical drift-tube support, the post couplers in the horizontal plane and the ion pumps below the cavities, the positions of other components are placed between 30° to 60° from the horizontal plane to avoid unwanted couplings to the post coupled structure and to allow all components (except bulk tuners) to be accessible and demountable from the outside.

Notes on Component Design

Drift Tubes. The short RF duty cycle ($< 2.2 \times 10^{-3}$) has allowed a simple design for drift-tube cooling via the support stem using the solid copper drift-tube shell to give the required heat transfer.

Girder Slot and Bulk Tuner. The bulk tuner with a "T" section of width w_b and height h_b perturbs the frequency as if it reduced the sectional area by

$$\delta A_b = w_b h_b + 2(k_b h_b^2) ,$$

where the second term represents the shadow effect on the H_ϕ field. Measurements on a model of Tank II gave values $k_b \approx 1.3$, so for a frequency perturbation +500 kHz (at 202.56 MHz), w_b = 50 mm and h_b = 35 mm are required. For the girder slot we would expect $A_s = W_s h_s - 2(k_s h_s^2)$ assuming that $w_s > 3h_s$, and we have measured $k_s \approx 1.0$. However, there is uncertainty in the slot region due to the drift-tube support stems. Until we have the cavities fully assembled, the final size of bulk tuner remains uncertain, but we estimate that a nominal bulk tuner perturbation of +500 kHz is required.

Piston Tuners. There is one piston tuner per tank section (10 total). At the normal RF duty cycle (0.6×10^{-3}) there will be two tuners per cavity for automatic frequency control, with the other on Tanks II and III used for manual setting-up.

RF Feed Loops. There are five coupling loops each corresponding to an RF amplifier and hence to 10 MeV acceleration. All loops are adjustable in area, to present a 50 Ω match to the amplifiers for all accelerated currents. The RF window is at $\sim \lambda/2$ from the loop.

RF Monitoring Loops. These are in air but couple to the H_ϕ field through pyrex thimbles spaced regularly (every four cells) along the accelerator.

Experimental Work on Post Couplers

The advantages of stabilized structures for improving transient response and easing of manufacturing tolerances are well documented[10], and in particular the post coupled structure is compatible with the single drift-tube support. We have extended the principle to lower energies, evaluated different post periodicities, and shown that a tilted field can also be stabilized. The first measurements were made on a 500 MHz model of the LAMPF Tank I (31 cells from 0.75 to 5 MeV) borrowed from LASL [a]. Axial fields were measured by frequency perturbation ("bead pull"). Field stability against large frequency shifts in end cells was demonstrated for one post coupler per drift tube (N=1), one per two drift tubes (N=2), and so on up to N=6. Successive posts were on alternate sides of the cavity. Although for the higher periodicities the axial field was less stable between the post

a) The generous help of D. Swenson and E. Schneider is gratefully acknowledged.

couplers, there were advantages in ease of setting-up and in increased spacing of the post coupler modes (which could provide the bandwidth limitation for the fast RF level control). For this short cavity ($L = 2.2\lambda$) the TM_{011} mode was displaced from $\sim$ 11 MHz to $\sim$ 17 MHz above the TM_{010} mode so that for the greatly improved stability the slope in the dispersion curves at the operating mode must be cited[11].

A study has been made of the post couplers, girder supports and other components on a 500 MHz model of Tank II. It was possible to operate both with a circular section cavity and then with a section like the actual cavity (Fig. 1). Initially the field distribution before stabilization was tolerably flat, but with the girders raised the field decreased by 53% along the cavity. With post couplers properly adjusted, we obtained the expected stabilized field. Stabilization was possible for coupler periodicities $N = 1$, 2 but not for $N \geq 3$. The $N = 2$ case was easier to stabilize, and for the longer cavity ($L = 8.8\lambda$) the normal mode spacing (TM_{010}-TM_{011}) of 0.59 MHz was increased to 2.63 and 2.53 MHz, for $N = 1$ and $N = 2$, respectively. For the actual linac we have chosen $N = 2$ for Tanks I and II and $N = 1$ for Tank III.

For Tank I the mean axial field must increase linearly along the tank by 21%. Measurements using the eccentric tabs on the posts showed that with all tabs pointing towards one end a significant field tilt could be obtained (e.g. for Tank II with $N = 2$, a field increase by $\times$ 2.6 from input to output). For adjustments under vacuum we prefer on Tank I an arrangement which rotates the post about a vertical axis at the cavity wall through $\pm 5^\circ$ in the horizontal plane. Stability is maintained over this range of rotation so we can set up the specified field tilt or other fields, e.g. for the acceleration of deuterons.

Although we obtained good stabilization of the field with the girders raised along the model cavity, measurements along the cavity showed large (5°) and periodic phase variations in H_ϕ due, it is assumed, to the post excitation necessary to counteract the unstabilized field errors. On the linac we will reduce the field errors with bulk tuners. (The phase of the axial electric field should be less affected by post excitation.)

Acknowledgements

The work reported in this paper could not have been done without the help of many people. Among them I would particularly like to thank M. Weiss for developing (with B. Bru) the vital matching concepts and tools used in the design procedure, I. White who was responsible for all model measurements reported here, and E. Boltezar for providing the mechanical engineering experience so necessary for the physical design. C. Poinard has contributed to the program improvements and has made most of the production runs.

References

1) D.J. Warner and M. Weiss, "Beam Optics in the CERN New 50 MeV Linac", to be published.

2) New Linac Working Group, "Project Study for a New 50 MeV Linear Accelerator for the CPS", CERN/MPS/LINP 73-1 (1973).

3) M. Martini and D.J. Warner, "Numerical Calculations of Linear Accelerator Cavities", CERN 68-11 (1968).

4) M. Martini and M. Promé, "Computer Studies of the Beam Dynamics in Proton Linear Accelerator with Space Charge", Particle Accelerators 2, 289 (1971).

5) M. Promé, "Effets de la charge d'espace dans les accélérateurs linéaires à protons", Dr. ès Sciences Thesis, Orsay (1971).

6) B. Bru and M. Weiss, "Linac Quadrupole Gradients and Matching Parameters at Different Beam Intensities", *in* Proc. 1970 Proton Linear Accel. Conf., Batavia (NAL, Batavia, 1971), p. 851.
B. Bru and M. Weiss, "Computational Methods and Computer Programs for Linearized Analysis of Periodic Structures", CERN/MPS/LIN 72-4 (1972).

7) B. Bru and D. Warner, "BUNCH 74, An Improved Multiparticle Beam Simulation Program", CERN/MPS/LIN 75-2 (1975).

8) B. Bru and M. Weiss, "Design of the Low Energy Beam Transport System for the New 50 MeV Linac", CERN/MPS/LIN 74-1 (1974).

9) D.J. Warner, "Accelerator Research and Development with the CERN 3 MeV Linac", *in* Proc. 1972 Proton Linear Accel. Conf., Los Alamos, p. 33.

10) G. Dome, "Review and Survey of Accelerating Structures", *in* "Linear Accelerators", eds. P. Lapostolle and A. Septier (North Holland, Amsterdam, 1970), pp. 637-738.

11) M. Bell, "On Stabilization of Linac Cavities", to be published.

TABLE I

STRUCTURE PARAMETERS

Parameter	Unit	Cavity No. I	Cavity No. II	Cavity No. III
Input energy	(MeV)	0.75	10.35	30.48
Output energy	(MeV)	10.35	30.48	50.00
Cavity length	(m)	6.939	12.958	13.359
Distance to next cavity	(m)	0.15	0.20	-
Cavity diameter	(m)	0.94	0.90	0.86
Number of unit cells		52	44	32
Number of post couplers		25	21	31
Drift tube diameter (d)	(mm)	180	160	160
Bore hole diameter (HD)	(mm)	20, 25	30	30
Upper profile radius (r)	(mm)	20	40	40
Lower profile radius (r_{hc})	(mm)	4, 5	10	10
Support stem diameter	(mm)	28	40	40
Post coupler diameter	(mm)	25	25	25
Gap/cell length g/L		0.222-0.314	0.201-0.294	0.262-0.316
Axial transit time factor (T)		0.676-0.804	0.873-0.835	0.865-0.816
Synchronous phase (ϕ_s)	(°)	(-35)-(-25)	-25	-25
Mean axial field ($\bar{E}$)	(MVm^{-1})	1.790-2.164	1.994	1.920
Peak surface field	(MVm^{-1})	10.0-9.3	12.6-9.6	10.0-9.7
Cavity RF power	(MW)	0.60	1.12	1.17
Beam RF for 150 mA	(MW)	1.44	3.02	2.93
Quadrupole effective length	(mm)	35,40,55,80	114	114
B′ for FD, μ = 39°, I = 150 mA	(Tm^{-1})	93-32	23-20	20-19

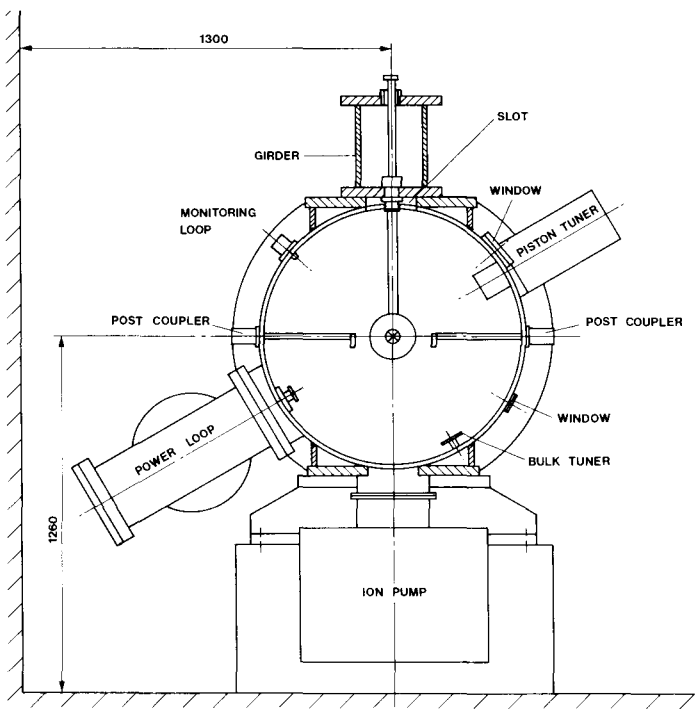

Fig. 1 Cavity cross section (schematic)